JCTC Journal of Chemical Theory and Computation

Induced-Polarization Energy Map: A Helpful Tool for Predicting Geometric Features of Anion-π Complexes

Daniel Escudero,[†] Antonio Frontera,*[,†] David Quiñonero,[†] Antoni Costa,[†] Pablo Ballester,[‡] and Pere M. Deyà*[,†]

Department of Chemistry, Universitat de les Illes Balears, Crta. de Valldemossa km 7.5, E-07122 Palma de Mallorca, Spain, and ICREA and Institute of Chemical Research of Catalonia (ICIQ), Avinguda Països Catalans 16, 43007 Tarragona, Spain

Received May 21, 2007

Abstract: In this manuscript we propose the use of a new tool that we have found useful to predict the geometries of ion-π complexes. This tool is entitled the Induced-Polarization Energy map (IPE map). The novelty of this representation is that in the map only the contribution of the ion-induced polarization term to the total interaction energy for a given noncovalent interaction is contoured in a 2D region. The IPE map has been found useful to predict and explain geometries of several complexes of a tetrahedral 2 anion (BF_4^-) with perfluoropyrazine, perfluoropyridazine, perfluoropyrimidine, the three isomers of perfluorotriazine, and the three isomers of perfluorotetrazine.

Introduction

In modern chemistry, noncovalent interactions are decisive. This is especially true in the field of supramolecular chemistry and molecular recognition.[1] In particular, interactions involving aromatic rings[2] are key processes in both chemical and biological recognition since aromatic rings are omnipresent in biological systems. A classical example is the interaction of cations with aromatic systems, namely cation-π interactions,[3] which are supposed to be decisive in the ion selectivity in potassium channels.[4] Such interactions are also important for the binding of acetylcholine to the active site of the enzyme acetylcholine esterase.[5] Recently, the importance of cation-π interactions in neurotransmitter receptors has been demonstrated,[6] and they play an important role in transport of nitrogen through the membrane by the ammonia transport protein.[7] Anion-π interactions[8] are also important noncovalent forces that have attracted considerable attention in the last 3 years. They have been observed experimentally, supporting the theoretical predictions and the promising proposal for the use of anion receptors based on anion-π interactions in molecular recognition.[9] In addition, π-acidic oligonaphthalendiimide rods have been recently proposed as transmembrane anion-π slides.[10] A recent review of P. Gamez et al. deals with anion-binding involving π-acidic heteroaromatic rings.[11]

The cation-π and anion-π interactions are mainly dominated by electrostatic and ion-induced polarization terms.[12] The nature of the electrostatic term can be rationalized by means of the permanent quadrupole moment of the arene. The face-to-face interaction of the benzene−hexafluorobenzene complex is favorable due to the large and opposite permanent quadrupole moments of the two molecules.[13] The $\pi-\pi$ interaction in the benzene dimer is governed by dispersion effects.[14] We have explained the dual binding mode of some molecules to form stable complexes with both cations and anions arguing polarization effects.[12c,15] Two examples are the triazine and trifluorobenzene rings, and the dual behavior is explained by means of the small quadrupole moment of these molecules. The interaction is thus dominated by polarization effects, and the electrostatic contribution to the interaction energy is negligible. As a consequence the binding energies of the complexes of these compounds with ions is small compared with benzene (cation-π complexes) or hexafluorobenzene (anion-π complexes), but recent reports have described the complexes formed between nitrate and the π face of triazine in solid phase.[16] Recently our group has published a theoretical MP2 study where the energetic and geometric characteristics of several π-complexes involv-

* Corresponding author: fax: +34 971 173426; e-mail: toni.frontera@uib.es (A.F.), pere.deya@uib.es (P.M.D.)
[†] Universitat de les Illes Balears.
[‡] ICIQ.

10.1021/ct700122y CCC: $37.00
Published on Web 10/11/2007

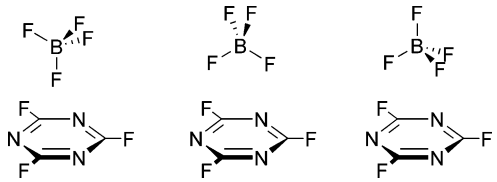

Figure 1. The three orientations of the complexes of trifluoro-*s*-triazine with BF_4^-.

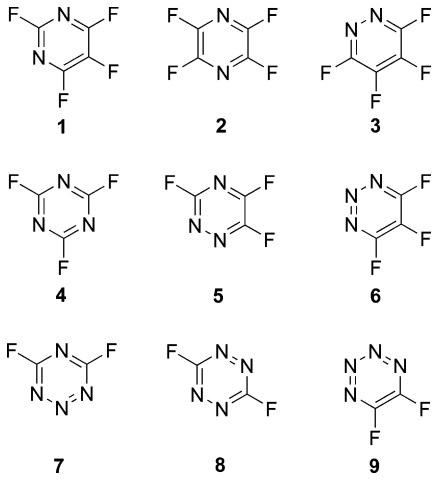

Figure 2. Perfluoropyrimidine (**1**), perfluoropyrazine (**2**), perfluoropyridazine (**3**), isomers of perflurotriazine (**4**−**6**), and isomers of perfluorotetrazine (**7**−**9**).

ing tetrahedral and octahedral anions have been analyzed and compared to X-ray structures retrieved from the Cambridge Structural Database.[17] In these complexes several orientations for the anion can be operative. For instance for the interaction of BF_4^- with perfluoro-*s*-triazine, the anion can interact with the aromatic ring using one, two, or three fluorine atoms (see Figure 1). In the present study, we propose the use of the Induced-Polarization Energy map (IPE map) as a useful tool to predict and explain the orientation of polyatomic anions in anion-π complexes, although it is expected that its use can be easily generalized to other systems such cation-π complexes.

In this manuscript we report a MP2 study, where we analyze complexes of the BF_4^- anion with perfluoropyrimidine (**1**), perfluoropyrazine (**2**), perfluoropyridazine (**3**), the three isomers of perfluorotriazine (**4**−**6**), and the three isomers of perfluorotetrazine (**7**−**9**) (see Figure 2). In addition we have computed the IPE maps for compounds **1**−**9** using the Molecular Interaction Potential with polarization (MIPp) partition scheme developed by Orozco and Luque.[18] The MIPp is a convenient tool for predicting binding properties. It has been successfully used for rationalizing molecular interactions such us hydrogen bonding and ion-π interactions and for predicting molecular reactivity.[19] The MIPp partition scheme is an improved generalization of the MEP where three terms contribute to the interaction energy: (i) an electrostatic term identical to the MEP,[20] (ii) a classical dispersion-repulsion term,[21] and (iii) a polarization term derived from perturbational theory.[22] The latter term has been used to construct the IPE maps, which has been compared to the MIPp maps. We have found that the geometric characteristics of the complexes of BF_4^- anion with compounds **1**−**9** are in agreement with the IPE maps, which are able to predict the orientation of the anion. This agreement confirms the importance of polarization effects in anion-π interactions not only energetically but also geometrically as well.

II. Theoretical Methods

The geometries of all compounds studied in this work were fully optimized using the MP2/6-31++G** level of theory within the Gaussian 03 package.[23] The minimum nature of the complexes was evaluated performing frequency analyses at the same level. In three complexes (**2**, **3**, and **7**) one small imaginary frequency has been found that corresponds to a rotational movement of the anion. The binding energies were calculated with correction for the basis set superposition error (BSSE) by using the Boys−Bernardi counterpoise technique.[24] The optimization of the complexes has been performed without imposing symmetry constraints unless otherwise noted. Calculation of the MIPp maps of **1**−**9** interacting with F^- was performed using the HF/6-31++G**//MP2/6-31++G** wave function by means of the MOPETE-98 program.[25] The ionic van de Waals parameters for F^- were taken from the literature.[26] Some basic concepts of MIPp follow (see refs 18 and 21 for a more comprehensive treatment). The MEP can be understood as the interaction energy between the molecular charge distribution and a classical point charge. The formalism used to derive MEP remains valid for any classical charge; therefore, it can be generalized using eq 1 where Q_B is the classical point charge at R_B. Q_B can adopt any value, but it has a chemical meaning only when $Q_B = 1$ (proton); ϕ stands for the set of basis functions used for the quantum mechanical molecule *A*; and $c_{\mu i}$ is the coefficient of atomic orbital μ in the molecular orbital *i*.

$$\mathrm{MEP} = \sum_A \frac{Z_A Q_B}{|R_B - R_A|} - \sum_i^{\mathrm{occ}} \sum_\mu \sum_\nu c_{\mu i} c_{\nu i} \left\langle \phi_\mu \left| \frac{Q_B}{|R_B - r|} \right| \phi_\nu \right\rangle \quad (1)$$

The MEP formalism permits the rigorous computation of the electrostatic interaction between any classical particle and the molecule. Nevertheless, nuclear repulsion and dispersion effects are omitted. This can be resolved by the addition of a classical dispersion-repulsion term, which leads to the definition of MIP[23] (eq 2), where *C* and *D* are empirical van der Waals parameters.

$$\mathrm{MIP} = \mathrm{MEP} + \sum_{A'B'} \left(\frac{C_{A'B'}}{|R_{B'} - R_{A'}|^{12}} - \frac{D_{A'B'}}{|R_{B'} - R_{A'}|^{6}} \right) \quad (2)$$

The definition of MIPp is given by eq 3, where polarization effects are included at the second-order perturbation level;[24] ϵ stands for the energy of virtual (*j*) and occupied (*i*) molecular orbitals. It is worth noting that eq 3 includes three important contributions: first, the rigorous calculation of electrostatic interactions between quantum mechanical and classical particles; second, the introduction of an empirical

Table 1. Binding Energies without and with the Basis Set Superposition Error Correction (E and E_{BSSE}, kcal/mol, Respectively) and Equilibrium Distances (R_e, Å, from the Boron Atom to the Ring Centroid) at the MP2/6-31++G** Level of Theory Computed for the Complexes of BF_4^- with Compounds **1**−**9**[a]

complex	E	E_{BSSE}	NImag	R_e	Q_{zz} (B)	α_z (au)
1+BF_4^-	−17.9	−13.2	0	3.37	8.9	33.0
2+BF_4^-	−16.5	−12.8	1	3.55	8.4	32.2
3+BF_4^-	−18.4	−13.6	1	3.41	8.4	32.6
4+BF_4^-	−17.1	−13.0	0	3.25	8.2	30.3
5+BF_4^-	−18.5	−13.9	0	3.45	8.8	30.5
6+BF_4^-	−19.4	−14.3	0	3.41	9.4	30.9
7+BF_4^-	−17.5	−13.6	1	3.51	8.7	27.7
8+BF_4^-	−18.3	−14.2	0	3.47	8.5	29.4
9+BF_4^-	−18.9	−14.4	0	3.56	9.5	28.6

[a] Several properties of compounds **1**−**9** are also included.

dispersion-repulsion term; and third, the perturbative treatment of the polarization term.

$$\mathrm{MIPp} = \mathrm{MIP} + \sum_{j}^{\mathrm{vir}} \sum_{i}^{\mathrm{occ}} \frac{1}{\epsilon_i - \epsilon_j} \left\{ \sum_{\mu} \sum_{\nu} c_{\mu i} c_{\nu i} \left\langle \phi_\mu \left| \frac{Q_B}{|R_B - r|} \right| \phi_\nu \right\rangle \right\}^2 \quad (3)$$

The "atoms-in-molecules" analysis[27] has been performed by means of the AIM2000 version 2.0 program[28] using the MP2/6-31++G** wave functions. The quadrupole moment of compounds **1**−**9** was computed using the CADPAC program[29] at the MP2/6-31G* level since previous studies[30] have demonstrated that quantitative results are obtained at this level of theory.

III. Results and Discussion

A. Energetic and Geometrical Results. In Table 1 we summarize the binding energies and equilibrium distances of the complexes of BF_4^- with compounds **1**−**9**. From the inspection of the results an interesting point arises. The interaction energy of perfluoroheteroaromatic compounds **1**−**9** with BF_4^- is large and negative, and its value is almost independent upon the number of the nitrogen atoms of the ring. This fact can be interpreted as a compensating effect, that is, the electron-withdrawing influence of a fluorine atom bonded to a carbon atom of the ring equals the atomic substitution of this carbon atom of the ring by one nitrogen atom, which is more electronegative than carbon. As a consequence, the π-acidity of the ring is essentially maintained. This fact can be corroborated by inspecting the values of quadrupole moments (Q_{zz}) and molecular polarizabilities (α_z), which have also been included in Table 1 for compounds **1**−**9**. As stated in the introduction, the physical nature of the anion-π interaction is mainly explained by the participation of two forces that contribute to the interaction: the electrostatic term and the ion-induced polarization. We have demonstrated that the former[12b] depends on the quadrupole moment of the aromatic compound (since the μ_z is negligible), and the latter depends on the molecular polarizability. The values of Q_{zz} and α_z present in Table 1 are comparable for all aromatic compounds and, thus, their interaction energies with BF_4^- are also comparable.

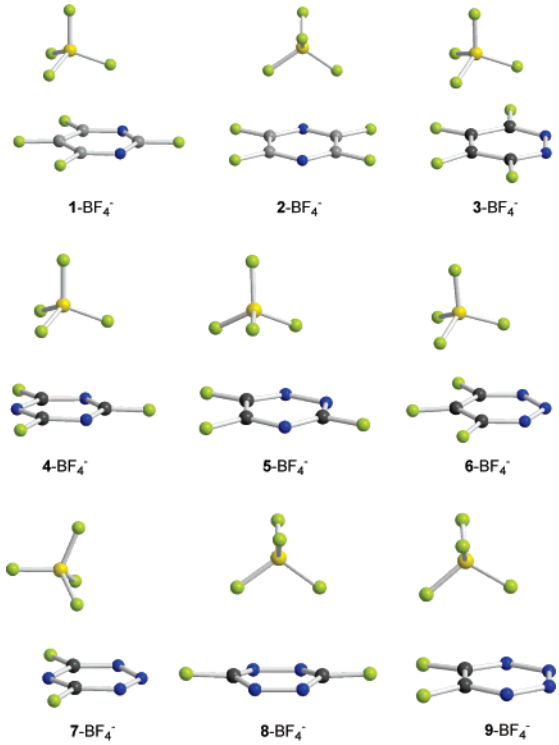

Figure 3. MP2/6-31++G** optimized structures of the π-complexes of BF_4^- with compounds **1**−**9**.

In Figure 3 we represent the MP2/6-31++G** optimized geometries of the anion-π complexes of compounds **1**−**9** interacting with BF_4^-. A variety of geometries is observed. In all cases the anion interacts with the π-cloud of the aromatic rings, but only in the more symmetric compounds the anion is located over the center of the ring (**2**, **4**, and **8**). In the other cases the anion is to some extent displaced from the ring centroid. In general the anion has the tendency to move over the region of the aromatic ring where a major number of carbon atoms is present (see Figure 3). The equilibrium distances observed for all complexes are similar, apart from complex **4**-BF_4^-. In this complex, the equilibrium distance (measured from boron atom to ring centroid) is shorter than the rest of complexes due to two factors. First, the boron atom is located over the center of the ring along the main symmetry axis. Second, in this complex three fluorine atoms of the anion are pointing at the ring. This geometry minimizes the distance from the boron atom to the ring centroid.

B. MIPp Analysis. We have performed the MIPp partition scheme calculation of compounds **1**−**9** interacting with F^- using the HF/6-31++G**//MP2/6-31++G** wave function. In the calculation F^- was considered as a classical nonpolarizable particle. The total MIPp energy is the sum of three terms, electrostatic, polarization, and van der Waals (dispersion-repulsion), as explained in the computational methods. We have computed bidimensional (2D) MIPp energy maps of compounds **1**−**9** interacting with F^- calculated at 2.6 Å above the molecular plane in order to explore their binding ability. In addition, using only the polarization contribution to the total MIPp energy, we have computed the 2D-IPE maps of compounds **1**−**9** interacting with F^- calculated at the same distance than the MIPp above the molecular plane. We have computed these maps to learn if this representation

Table 2. Interaction Energies (kcal/mol) Computed at the MIPp and IPE Minima Observed for Compounds **1**−**9** Interacting with F^{-a}

compound	MIPp	IPE	%IPE (%)
1	−22.2	−12.0	54
2	−22.1	−11.7	52
3	−21.5	−12.1	56
4	−23.0	−10.3	44
5	−22.8	−11.1	49
6	−21.5	−11.7	54
7	−23.2	−10.0	43
8	−22.2	−10.2	46
9	−22.4	−10.7	48

[a] The percentage of the polarization term to the total interaction energy is also shown.

can be useful to predict the geometric characteristics of anion-π complexes, especially when the anion is polyatomic. Bearing in mind that the anion-π interaction is mainly characterized by electrostatic and ion-induced polarization forces and that electrostatic forces are not directional, a mapping of the polarization contribution can give valuable information about the position of the anion over the aromatic ring. For all compounds the energetic value of the MIPp measured at the minimum ranges from −23.2 to −21.5 kcal/mol and the one for the IPE ranges from −12.0 to −10.0 kcal/mol (see Table 2), in agreement with the values of Q_{zz} and α_z of **1**−**9** (see Table 1). This result confirms that the polarization term is important, and its contribution accounts for approximately 50% of the total interaction energy. Previous studies[8a,9e,12b,c,15,17] demonstrate that the MIPp energies are in agreement with the interaction energies measured optimizing the complexes at the MP2 level of theory, which give reliability to the MIPp partition scheme. In the complexes studied in this work, a direct comparison of the MIPp energy values and the MP2/6-31++G** interaction energies is not possible, since the MIPp maps are computed using F^- as the interacting particle instead of BF_4^-. The interaction energies present in Table 1 are lower than the MIPp values present in Table 2, because the formal charge assigned to the interacting particle is "−1" and the formal charge of the fluorine atoms of the BF_4^- anion is smaller. We have computed the 2D-IPE and 2D-MIPp maps 2.6 Å above the molecular plane because this is the location of the MIPp minimum when a F^- approaches the center of the ring of compounds **1**−**9** following a perpendicular trajectory.

1. Heteroaromatic Rings with Two Nitrogen Atoms. The 2D-IPE(F^-) maps of perfluoropyrimidine (**1**), perfluoropyrazine (**2**), and perfluoropyridazine (**3**) are represented in Figures 4−6. In addition the 2D-MIPp(F^-) maps are represented in the figures for comparison purposes. The corresponding MP2/6-31++G** optimized complexes are also included in the figures in order to illustrate the agreement of the 2D-IPE/MIPp maps with the geometric features of the complexes. For compounds **1**−**3** the 2D-MIPp maps predict a minimum on the potential energy located approximately over the center of the ring. In contrast the 2D-IPE maps show a totally different distribution. For instance, the 2D-IPE map of compound **1** (see Figure 4) predicts a minimum which is located over the region of C5. The optimized geometry of the **1**-BF_4^- complex is in total agreement with the location of the IPE minimum. In addition, the geometry of the complex is not in disagreement with the 2D-MIPp map since one fluorine atom of the BF_4^- anion is located near the MIPp minimum.

The plots of 2D-IPE(F^-) and 2D-MIPp(F^-) maps computed for **2** are represented in Figure 5. The position of the anion is in accord with the MIPp map, since it is located

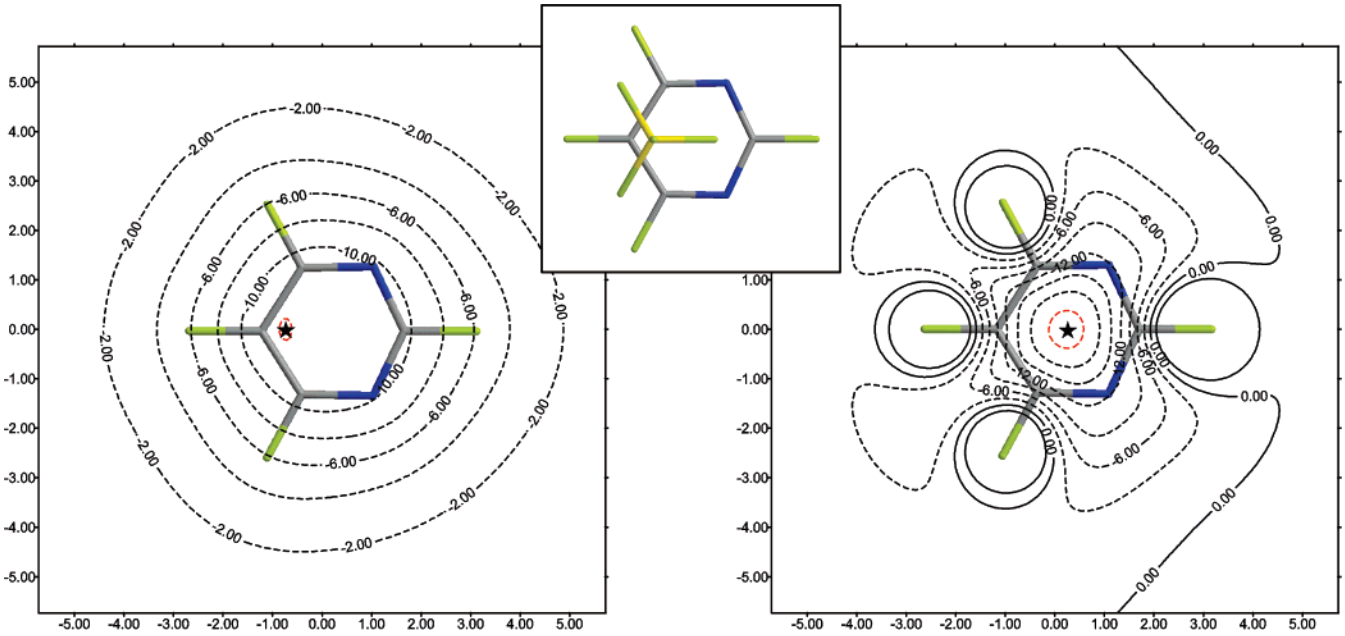

Figure 4. Left: 2D-IPE(F^-) map computed at 2.6 Å. Isocontour lines are drawn every 2 kcal/mol. The red isocontour corresponds to −12 kcal/mol. The minimum is represented by a star. Right: The 2D-MIPp(F^-) map is computed at 2.6 Å above the molecular plane. Isocontour lines are drawn every 3 kcal/mol, solid lines correspond to positive values of energy, and dashed lines correspond to negative values. The red isocontour line corresponds to −21 kcal/mol. The minimum is represented by a star. Middle: A zenithal view of the optimized **1**-BF_4^- complex is represented (MP2/6-31++G**).

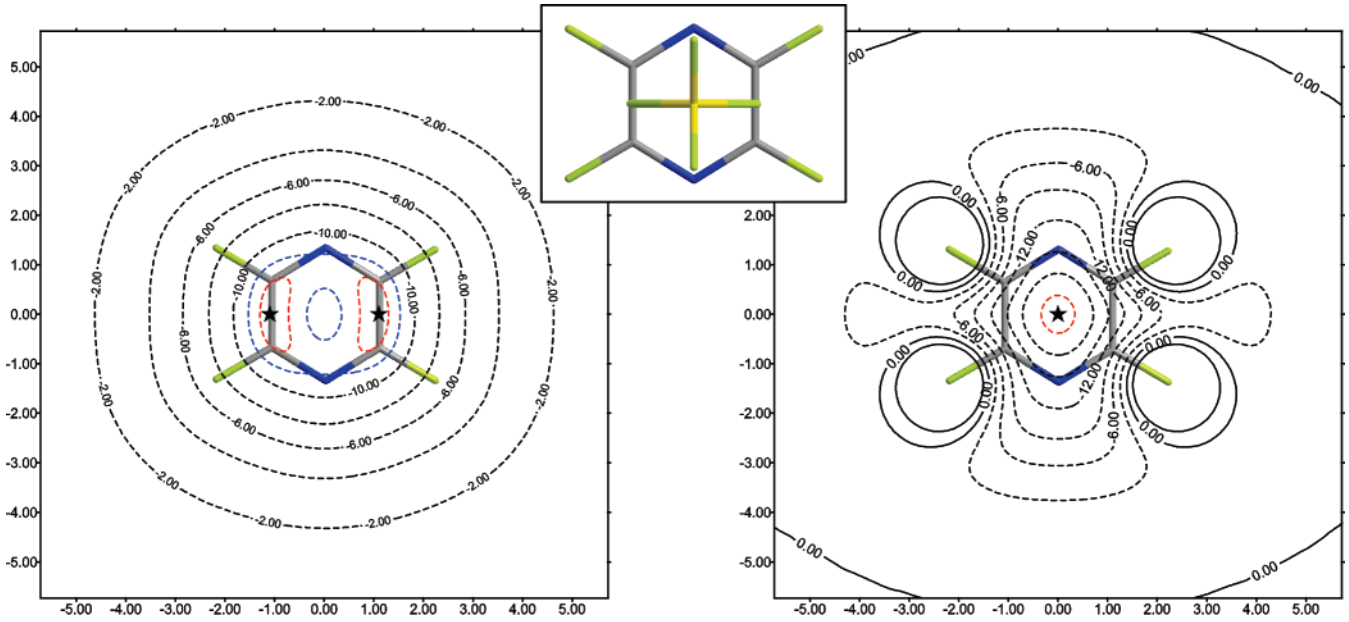

Figure 5. Left: 2D-IPE(F^-) map computed at 2.6 Å. Isocontour lines are drawn every 2 kcal/mol. The blue isocontour corresponds to −11 kcal/mol, and the red isocontour corresponds to −11.5 kcal/mol. The minima are represented by stars. Right: The 2D-MIPp(F^-) map is computed at 2.6 Å above the molecular plane. Isocontour lines are drawn every 3 kcal/mol, solid lines correspond to positive values of energy, and dashed lines correspond to negative values. The red isocontour line corresponds to −21 kcal/mol. The minimum is represented by a star. Middle: A zenithal view of the optimized **2**-BF_4^- complex is represented (MP2/6-31++G**).

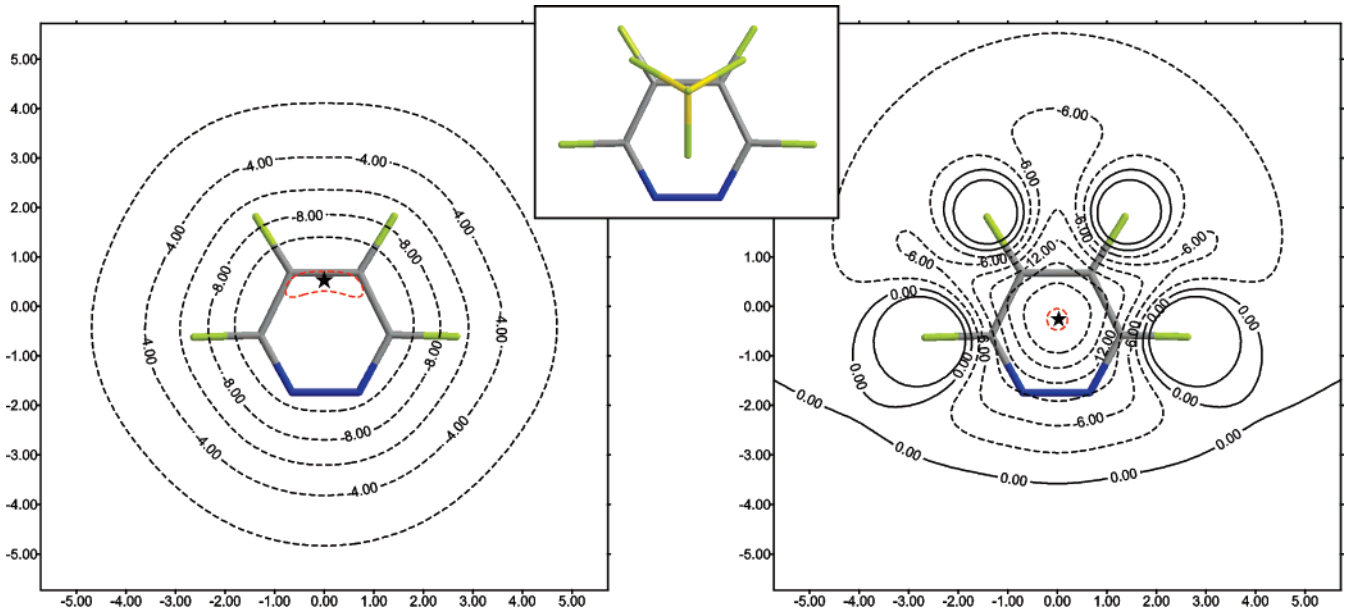

Figure 6. Left: 2D-IPE(F^-) map computed at 2.6 Å. Isocontour lines are drawn every 2 kcal/mol. The red isocontour corresponds to −12 kcal/mol. The minimum is represented by a star. Right: The 2D-MIPp(F^-) map is computed at 2.6 Å above the molecular plane. Isocontour lines are drawn every 3 kcal/mol, solid lines correspond to positive values of energy, and dashed lines correspond to negative values. The red isocontour line corresponds to −21 kcal/mol. The minimum is represented by a star. Middle: A zenithal view of the optimized **3**-BF_4^- complex is represented (MP2/6-31++G**).

over the center of the ring. As expected, there is a good agreement between the location of two fluorine atoms of the anion and the position of the two minima found in the 2D-IPE(F^-) map. In the optimized complex **2**-BF_4^- two fluorine atoms of the BF_4^- are pointing to the middle of two C−C bonds, precisely where the IPE minima are found.

The plots of 2D-IPE(F^-) and 2D-MIPp(F^-) maps computed for **3** are represented in Figure 6. The IPE minimum is located over the middle of the C4−C5 bond, and the MIPp minimum is located approximately over the center of the ring, to a minor extent displaced toward the C4−C5 region. The MP2/6-31++G** optimized structure of the **3**-BF_4^- complex is in agreement with both maps. The anion is approximately located where the IPE map predicts with one fluorine atom located at the MIPp minimum. For compounds **2** and **3** (Figures 5 and 6) the 2D-IPE and 2D-MIPp maps

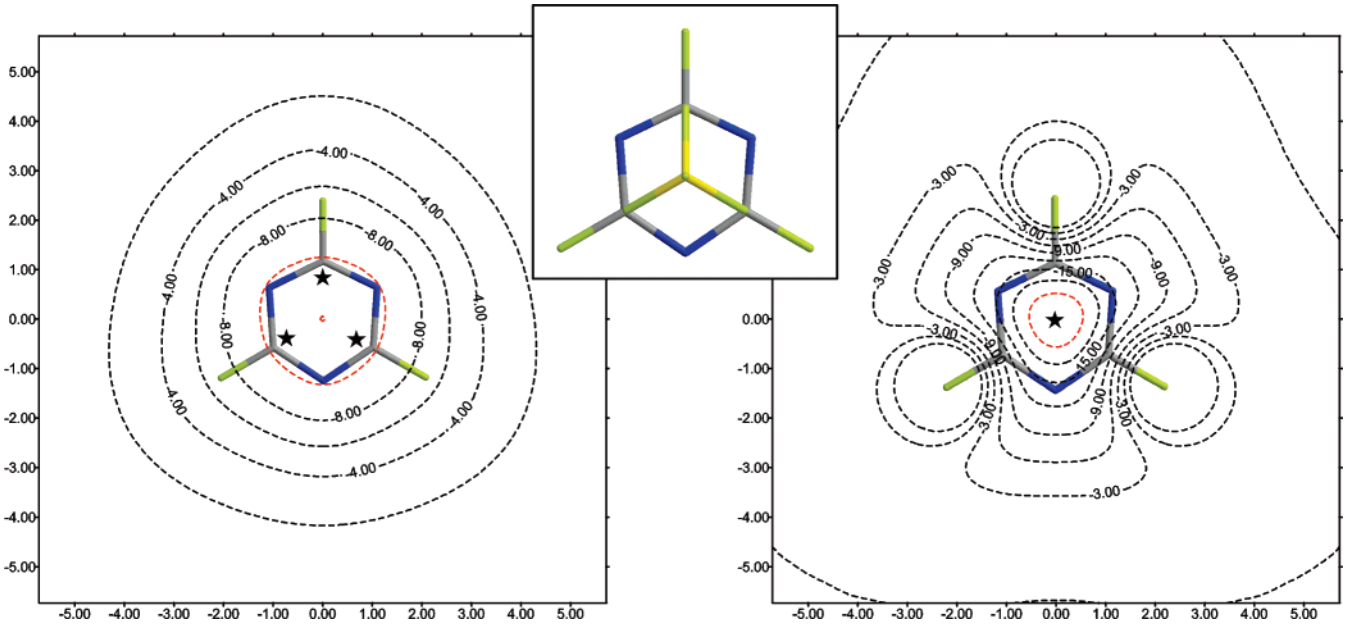

Figure 7. Left: IPE(F^-) map computed at 2.6 Å. Isocontour lines are drawn every 2 kcal/mol. The red isocontour corresponds to −10 kcal/mol. The minima are represented by stars. Right: The 2D-MIPp(F^-) map is computed at 2.6 Å above the molecular plane. Isocontour lines are drawn every 3 kcal/mol, solid lines correspond to positive values of energy, and dashed lines correspond to negative values. The red isocontour line corresponds to −21 kcal/mol. The minimum is represented by a star. Middle: A zenithal view of the optimized **4**-BF_4^- complex is represented (MP2/6-31++G**).

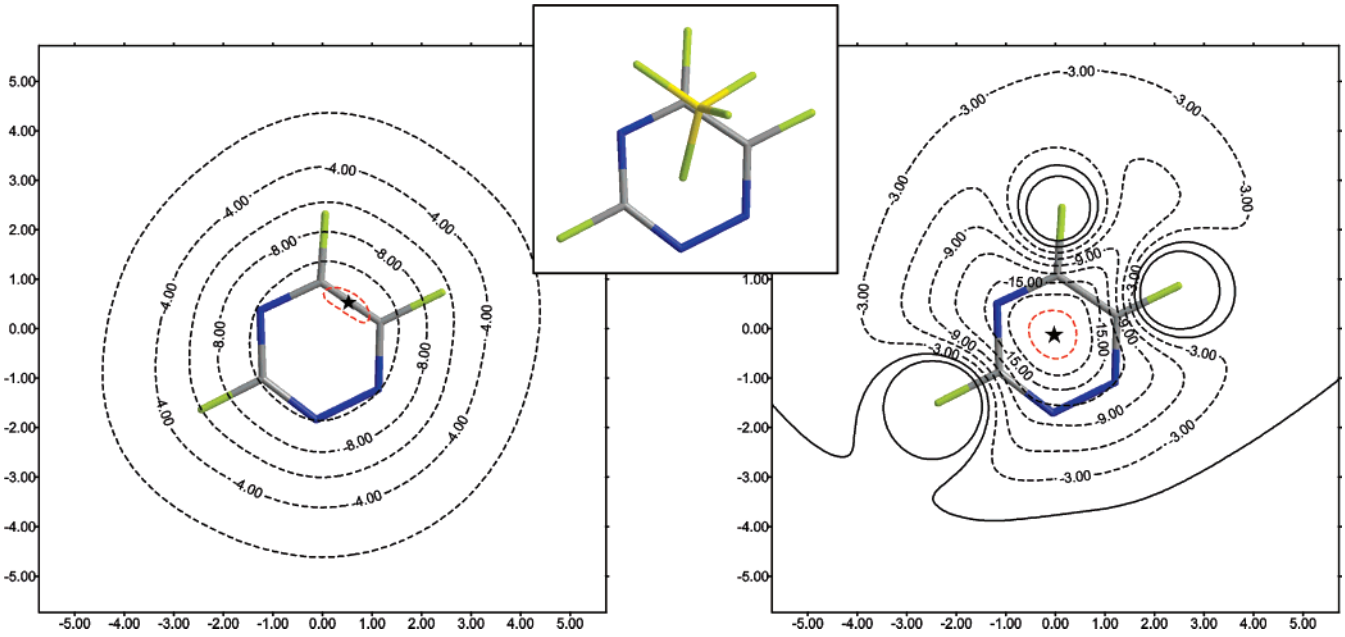

Figure 8. Left: IPE(F^-) map computed at 2.6 Å. Isocontour lines are drawn every 2 kcal/mol from −2.0 to 10.0 kcal/mol. The red isocontour corresponds to −11 kcal/mol. The minimum is represented by a star. Right: The 2D-MIPp(F^-) map is computed at 2.6 Å above the molecular plane. Isocontour lines are drawn every 3 kcal/mol, solid lines correspond to positive values of energy, and dashed lines correspond to negative values. The red isocontour line corresponds to −21 kcal/mol. The minimum is represented by a star. Middle: A zenithal view of the optimized **5**-BF_4^- complex is represented (MP2/6-31++G**).

nicely complement each other and are useful tools to explain the observed geometric features of the optimized complexes.

2. Heteroaromatic Compounds with Three Nitrogen Atoms. The 2D-IPE(F^-) and 2D-MIPp maps of the three isomers of perfluorotriazine (**4**−**6**) are represented in Figures 7−9. In addition, the optimized complexes are also represented in the figures for comparison purposes. For trifluoro-*s*-triazine **4** the IPE and MIPp maps are depicted in Figure 7. The location of the minima at the 2D-IPE map and the geometry of the optimized complex are in good agreement. There are three IPE minima, and their position coincides with the location of three fluorine atoms of the anion. In this case both maps are useful, since the location of the BF_4^- anion agrees with the 2D-MIPp map (over the center of the ring)

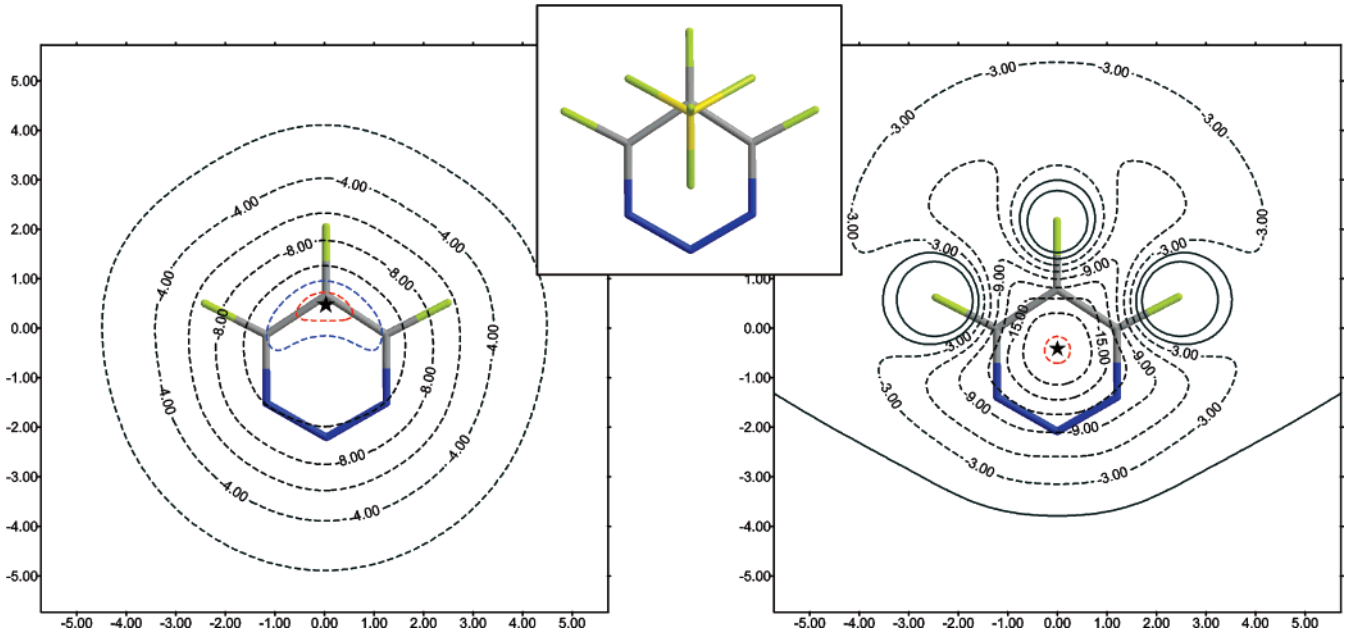

Figure 9. Left: IPE(F^-) map computed at 2.6 Å. Isocontour lines are drawn every 2 kcal/mol from −2.0 to −10.0 kcal/mol. The blue isocontour corresponds to −11.0 kcal/mol, and the red isocontour corresponds to −11.5 kcal/mol. The minimum is represented by a star. Right: The 2D-MIPp(F^-) map is computed at 2.6 Å above the molecular plane. Isocontour lines are drawn every 3 kcal/mol, solid lines correspond to positive values of energy, and dashed lines correspond to negative values. The red isocontour line corresponds to −21 kcal/mol. The minimum is represented by a star. Middle: A zenithal view of the optimized **6**-BF_4^- complex is represented (MP2/6-31++G**).

and the orientation of the anion agrees with the 2D-IPE map (three F atoms pointing to the ring).

The 2D-IPE and 2D-MIPp maps computed for 1,2,4-trifluorotriazine (**5**) are represented in Figure 8. The position of the anion in the **5**-BF_4^- complex agrees with the location of the IPE minimum. In addition the position of one fluorine atom of the anion agrees with the MIPp minimum. A parallel finding has been found for 1,2,3-trifluorotriazine **6** (see Figure 9); the position of the anion in the **6**-BF_4^- complex agrees with the IPE minimum, and the position of one fluorine atom of the anion agrees with the MIPp minimum. These results confirm the utility of the IPE maps to predict the geometries of anion-π complexes of asymmetric aromatic compounds and that they usefully complement the MIPp maps.

3. Heteroaromatic Compounds with Four Nitrogen Atoms. The 2D-IPE(F^-) and 2D-MIPp maps of the three isomers of perfluorotetrazine (**7**−**9**) and the geometry of the optimized complexes of compounds **7**−**9** with BF_4^- are represented in Figures 10−12. The 2D-IPE(F^-) map of 1,2,3,5-tetrazine **7** is in sharp agreement with the optimized geometry of the complex, as can be observed in Figure 10. Two fluorine atoms of the anion are located at the IPE minima. In this case the position of the anion is not in total agreement with the MIPp minimum, nevertheless the spatial location of the BF_4^- is approximately on the region of the red contour.

The 2D-IPE(F^-) and 2D-MIPp(F^-) maps of 1,2,4,5-perfluorotetrazine **8** are shown in Figure 11. As expected, the agreement between both maps and the geometry of the complex is good. The location of two fluorine atoms of the anion agrees with the IPE minima, and the global location of the BF_4^- anion agrees with the MIPp minimum. This behavior has also been observed for the other symmetric complexes **2**-BF_4^- and **4**-BF_4^- (see Figures 5 and 7, respectively), for which the IPE map accurately predicts and explains the orientation of the anion and the MIPp explains the position of the anion.

The 2D-IPE(F^-) and 2D-MIPp(F^-) maps computed for 1,2,3,4-perfluorotetrazine (**9**) are represented in Figure 12. The position of the anion in the **9**-BF_4^- complex agrees with the location of the IPE minimum, and the position of one fluorine atom of the anion agrees with the MIPp minimum. A similar behavior has been observed for the complexes of low symmetry (C_s or C_1), i.e. complexes of compounds **1**, **3**, **5**, and **6**.

C. AIM Analysis. We have used the Bader's theory of "atoms-in-molecules" (AIM), which has been widely used to characterize a great variety of interactions,[31] to analyze the anion-π interaction of the complexes and to study if there is a relationship between the location of critical points and the IPE and MIPp minima. It has been demonstrated that the value of the electron charge density at the (3,+3) critical point (CP) that it is generated in anion-π complexes can be used as a measure of the bond order.[12b,c] In addition, the presence of bond critical points between the anion and the atoms of the ring is a clear indication of bonding.[27] In Figure 13 we show the distribution of (3,-1) and (3,+3) CPs in complexes **2**-BF_4^-, **4**-BF_4^-, and **8**-BF_4^-. We have chosen the symmetric complexes to illustrate the distribution of CPs for the sake of clarity. Moreover the ring CPs are not shown for the same reason. The other complexes exhibit a more complicated distribution of CPs, and they have been included in the Supporting Information (Figures S1−S3). For complex **2**-BF_4^-, the exploration of the CPs revealed the presence of two (3, −1) and one (3, +3) CPs. The bond CPs connect two fluorine atoms of the anion with the middle of two C−C

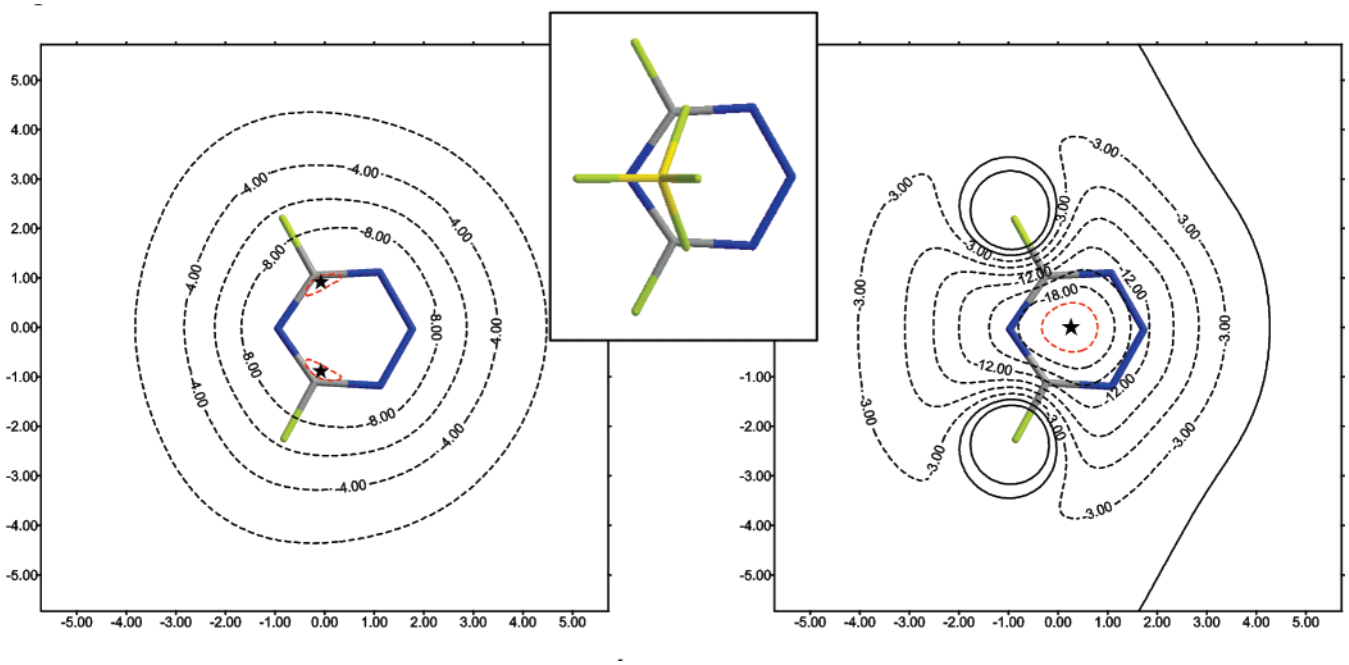

Figure 10. Left: IPE(F^-) map computed at 2.6 Å. Isocontour lines are drawn every 2 kcal/mol from −2.0 to −10.0 kcal/mol. The red isocontour corresponds to −10 kcal/mol. The minima are represented by stars. Right: The 2D-MIPp(F^-) map is computed at 2.6 Å above the molecular plane. Isocontour lines are drawn every 3 kcal/mol, solid lines correspond to positive values of energy, and dashed lines correspond to negative values. The red isocontour line corresponds to −21 kcal/mol. The minimum is represented by a star. Middle: A zenithal view of the optimized **7**-BF_4^- complex is represented (MP2/6-31++G**).

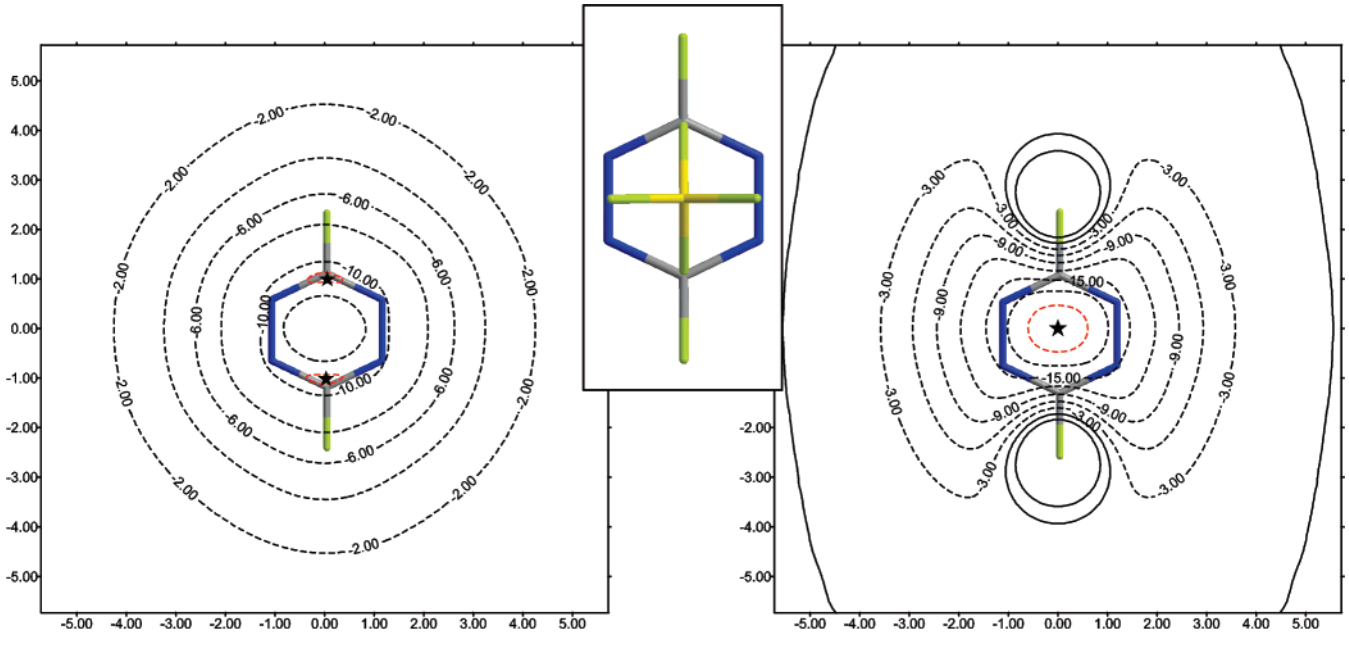

Figure 11. Left: IPE(F^-) map computed at 2.6 Å. Isocontour lines are drawn every 2 kcal/mol from −2.0 to −10.0 kcal/mol. The red isocontour corresponds to −10.2 kcal/mol. The minima are represented by stars. Right: The 2D-MIPp(F^-) map is computed at 2.6 Å above the molecular plane. Isocontour lines are drawn every 3 kcal/mol, solid lines correspond to positive values of energy, and dashed lines correspond to negative values. The red isocontour line corresponds to −21 kcal/mol. The minimum is represented by a star. Middle: A zenithal view of the optimized **8**-BF_4^- complex is represented (MP2/6-31++G**).

bonds, and the cage CP connects the boron atom of the anion with the center of the aromatic ring. For complex **4**-BF_4^-, the exploration of the CPs revealed the presence of three (3, −1) and one (3, +3) CPs. The bond CPs connect three fluorine atoms of the anion with the carbon atoms of the ring, and the cage CP connects the boron atom of the anion with the ring centroid. For complex **8**-BF_4^-, the exploration of the CPs revealed the presence of two (3, −1) and one (3, +3) CPs. The bond CPs connect two fluorine atoms of the anion with the carbon atoms of the ring, and the cage CP connects the boron atom of the anion with the ring centroid. This distribution of CPs observed for the **2**-BF_4^-, **4**-BF_4^-,

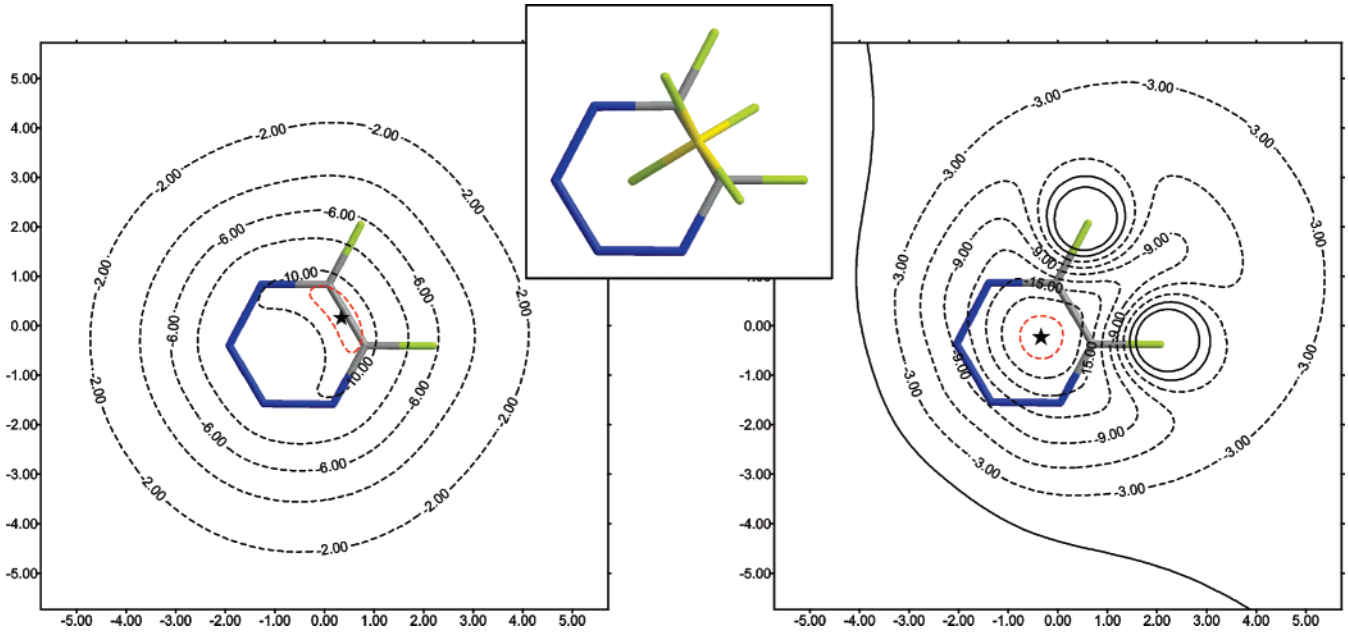

Figure 12. Left: IPE(F^-) map computed at 2.6 Å. Isocontour lines are drawn every 2 kcal/mol from −2.0 to −10.0 kcal/mol. The red isocontour corresponds to −10.5 kcal/mol. The minimum is represented by a star. Right: The 2D-MIPp(F^-) map is computed at 2.6 Å above the molecular plane. Isocontour lines are drawn every 3 kcal/mol, solid lines correspond to positive values of energy, and dashed lines correspond to negative values. The red isocontour line corresponds to −21 kcal/mol. The minimum is represented by a star. Middle: A zenithal view of the optimized **9**-BF_4^- complex is represented (MP2/6-31++G**).

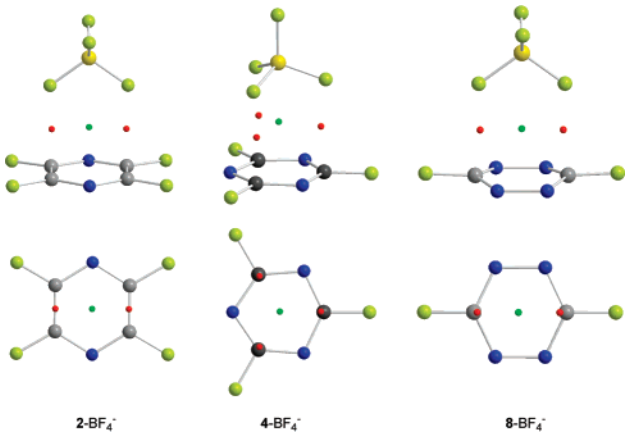

Figure 13. Schematic representation of the location of the (3,-1) bond CPs (red circles) and (3,+3) CP (green circle) originated upon complexation of the anion with compounds **2** (left), **4** (middle), and **8** (right). On the bottom the complexes are viewed perpendicular to the aromatic ring; for clarity, the anion has been omitted.

and **8**-BF_4^- is in good agreement with the 2D-IPE and 2D-MIPp maps and the location of the minima. The position of the bond CPs is related to the location of the IPE minima, and the position of the cage CPs corresponds to the location of the MIPp minima. For the rest of the complexes an acceptable agreement between the distribution of bond and cage CPs and the location of the IPE and MIPp minima is also found (see the Supporting Information), which is better for the C_s complexes **1**-BF_4^-, **3**-BF_4^-, **7**-BF_4^-, and **9**-BF_4^- than for complex **5**-BF_4^-. As aforementioned, the distribution of CPs is complicated, and, in general, the concentration of bond and cage CPs are mainly placed in the regions of the IPE and MIPp minima (see Figures S1−S3).

IV. Conclusion

The results derived from this study reveal that the 2D-IPE map is a good tool to predict and explain the geometric features of anion-π complexes. The polarization contribution to the total interaction energy is similar in magnitude to the electrostatic term. Moreover, it is more directional and is decisive to control the orientation of the tetrahedral BF_4^- anion.

The agreement between the MP2/6-31++G** optimized complexes and the 2D-IPE maps gives reliability to the MIPp partition scheme and supports the importance of polarization effects in both energetic and geometric characteristics of anion-π interactions. For symmetric complexes (C_{3v} and C_{2v}) the IPE map predicts the spatial disposition of the fluorine atoms, and the MIPp map predicts the position of the BF_4^-. For the rest of complexes the IPE map predicts the position of the BF_4^- anion, and the MIPp minimum coincides with the position of one fluorine atom of the anion. Finally, the AIM analysis is consistent with the IPE and MIPp maps.

Acknowledgment. We thank the DGICYT of Spain (projects CTQ2005-08989-01 and CTQ2005-08989-02) for financial support. We thank the CESCA for computational facilities. D.E. thanks the MEC for an undergraduate fellowship. D.Q. thanks the MEC for a "Juan de la Cierva" contract.

Supporting Information Available: Cartesian coordinates of MP2/6-31++G** optimized complexes and figures of AIM analysis of complexes of BF_4^- with compounds **1**, **3**, **5**−**7**, and **9** (Figures S1−S3). This material is available free of charge via the Internet at http://pubs.acs.org.

References

(1) Hunter, C. A.; Sanders, J. K. M. *J. Am. Chem. Soc.* **1990**, *112*, 5525.

(2) Meyer, E. A.; Castellano, R. K.; Diederich, F. *Angew. Chem., Int. Ed*. **2003**, *42*, 1210.

(3) (a) Ma, J. C.; Dougherty, D. A. *Chem. Rev*. **1997**, *97*, 1303. (b) Gallivan, J. P.; Dougherty, D. A. *Proc. Natl. Acad. Sci. U.S.A.* **1999**, *96*, 9459. (c) Gokel, G. W.; Wall, S. L. D.; Meadows, E. S. *Eur. J. Org. Chem*. **2000**, 2967. (d) Gokel, G. W.; Barbour, L. J.; Wall, S. L. D.; Meadows, E. S. *Coord. Chem. Rev*. **2001**, *222*, 127. (e) Gokel, G. W.; Barbour, L. J.; Ferdani, R.; Hu, J. *Acc. Chem. Res.* **2002**, *35*, 878. (f) Hunter, C. A.; Singh, J.; Thorton, J. M. *J. Mol. Biol*. **1991**, *218*, 837.

(4) (a) Kumpf, R. A.; Dougherty, D. A. *Science* **1993**, *261*, 1708. (b) Heginbotham, L.; Lu, Z.; Abramson, T.; Mackinnon, R. *Biophys. J.* **1994**, *66*, 1061.

(5) Dougherty, D. A. *Science* **1996**, *271*, 163.

(6) Lummis, S. C. R.; Beene, D. L.; Harrison, N. J.; Lester, H. A.; Dougherty, D. A. *Chem. Biol*. **2005**, *12*, 993.

(7) Ishikita, H.; Knapp, E.-W. *J. Am. Chem. Soc*. **2007**, *129*, 1210.

(8) (a) Quiñonero, D.; Garau, C.; Rotger, C.; Frontera, A.; Ballester, P.; Costa, A.; Deyà, P. M. *Angew. Chem., Int. Ed*. **2002**, *41*, 3389. (b) Alkorta, I.; Rozas, I.; Elguero, J. *J. Am. Chem. Soc*. **2002**, *124*, 8593. (c) Mascal, M.; Armstrong, A.; Bartberger, M. *J. Am. Chem. Soc*. **2002**, *124*, 6274.

(9) (a) Demeshko, S.; Dechert, S.; Meyer, F. *J. Am. Chem. Soc*. **2004**, *126*, 4508. (b) Schottel, B. L.; Bacsa, J.; Dunbar, K. R. *Chem. Commun*. **2005**, 46. (c) Rosokha, Y. S.; Lindeman, S. V.; Rosokha, S. V.; Kochi, J. K. *Angew. Chem., Int. Ed*. **2004**, *43*, 4650. (d) de Hoog, P.; Gamez, P.; Mutikainen, I.; Turpeinen, U.; Reedijk, J. *Angew. Chem., Int. Ed*. **2004**, *43*, 5815. (e) Frontera, A.; Saczewski, F.; Gdaniec, M.; Dziemidowicz-Borys, E.; Kurland, A.; Deyà, P. M.; Quiñonero, D.; Garau, C. *Chem. Eur. J*. **2005**, *11*, 6560. (f) Gil-Ramirez, G.; Benet-Buchholz, J.; Escudero-Adan, E. C.: Ballester, P. *J. Am. Chem. Soc*. **2007**, *129*, 3820. (g) Mascal, M. *Angew. Chem., Int. Ed*. **2006**, *45*, 2890.

(10) Gorteau, V.; Bollot, G.; Mareda, J.; Perez-Velasco, A.; Matile, S. *J. Am. Chem. Soc*. **2006**, *128*, 14788.

(11) Gamez, P.; Mooibroek, T. J.; Teat, S. J.; Reedijk, J. *Acc. Chem. Res*. **2007**, *40*, 435.

(12) (a) Cubero, E.; Luque, F. J.; Orozco, M. *Proc. Natl. Acad. Sci. U.S.A*. **1998**, *95*, 5976. (b) Garau, C.; Frontera, A.; Quiñonero, D.; Ballester, P.; Costa, A.; Deyà, P. M. *ChemPhysChem* **2003**, *4*, 1344. (c) Garau, C.; Frontera, A.; Quiñonero, D.; Ballester, P.; Costa, A.; Deyà, P. M. *J. Phys. Chem. A* **2004**, *108*, 9423.

(13) (a) Williams, J. H.; Cockcroft, J. K.; Fitch, A. N. *Angew. Chem., Int. Ed. Engl*. **1992**, *31*, 1655. (b) Williams, J. H. *Acc. Chem. Res*. **1993**, *26*, 593. (c) Adams, H.; Carver, F. J.; Hunter, C. A.; Morales, J. C.; Seward, E. M. *Angew. Chem., Int. Ed. Engl*. **1996**, *35*, 1542.

(14) Sinnokrot, M. O.; Sherrill, C. D. *J. Phys. Chem. A* **2004**, *108*, 10200.

(15) (a) Garau, C.; Quiñonero, D.; Frontera, A.; Ballester, P.; Costa, A.; Deyà, P. M. *Org. Lett*. **2003**, *5*, 2227. (b) Quiñonero, D.; Garau, C.; Frontera, A.; Ballester, P.; Costa, A.; Deyà, P. M. *Chem. Phys. Lett*. **2002**, *359*, 486.

(16) (a) Maheswari, P. U.; Modec, B.; Pevec, A.; Kozlevcar, B.; Massera, C.; Gamez, P.; Reedijk, J. *Inorg. Chem.* **2006**, *45*, 6637. (b) Mooibroek, T. J.; Gamez, P. *Inorg. Chim. Acta* **2007**, *360*, 381.

(17) (a) Garau, C.; Quiñonero, D.; Frontera, A.; Escudero, D.; Ballester, P.; Costa, A.; Deyà, P. M. *Chem. Phys. Lett*. **2007**, *438*, 104. (b) Quiñonero, D.; Frontera, A.; Escudero, D.; Ballester, P.; Costa, A.; Deyà, P. M. *ChemPhysChem* **2007**, *8*, 1182.

(18) Luque, F. J.; Orozco, M. *J. Comput. Chem*. **1998**, *19*, 866.

(19) (a) Hernández, B.; Orozco, M.; Luque, F. J. *J. Comput.-Aided Mol. Des*. **1997**, *11*, 153. (b) Luque, F. J.; Orozco, M. *J. Chem. Soc., Perkin Trans. 2* **1993**, 683. (c) Quiñonero, D.; Frontera, A.; Suner, G. A.; Morey, J.; Costa, A.; Ballester, P.; Deyà, P. M.; *Chem. Phys. Lett*. **2000**, *326*, 247. (d) Quiñonero, D.; Frontera, A.; Garau, C.; Ballester, P.; Costa, A.; Deyà P. M. *ChemPhysChem*. **2006**, *7*, 2487.

(20) Scrocco, E.; Tomasi, J. *Top. Curr. Chem*. **1973**, *42*, 95.

(21) Orozco, M.; Luque, F. J. *J. Comput. Chem*. **1993**, *14*, 587.

(22) Francl, M. M. *J. Phys. Chem*. **1985**, *89*, 428.

(23) Frisch, M. J.; Trucks, G. W.; Schlegel, H. B.; Scuseria, G. E.; Robb, M. A.; Cheeseman, J. R.; Montgomery, J. A., Jr.; Vreven, T.; Kudin, K. N.; Burant, J. C.; Millam, J. M.; Iyengar, S. S.; Tomasi, J.; Barone, V.; Mennucci, B.; Cossi, M.; Scalmani, G.; Rega, N.; Petersson, G. A.; Nakatsuji, H.; Hada, M.; Ehara, M.; Toyota, K.; Fukuda, R.; Hasegawa, J.; Ishida, M.; Nakajima, T.; Honda, Y.; Kitao, O.; Nakai, H.; Klene, M.; Li, X.; Knox, J. E.; Hratchian, H. P.; Cross, J. B.; Adamo, C.; Jaramillo, J.; Gomperts, R.; Stratmann, R. E.; Yazyev, O.; Austin, A. J.; Cammi, R.; Pomelli, C.; Ochterski, J. W.; Ayala, P. Y.; Morokuma, K.; Voth, G. A.; Salvador, P.; Dannenberg, J. J.; Zakrzewski, V. G.; Dapprich, S.; Daniels, A. D.; Strain, M. C.; Farkas, O.; Malick, D. K.; Rabuck, A. D.; Raghavachari, K.; Foresman, J. B.; Ortiz, J. V.; Cui, Q.; Baboul, A. G.; Clifford, S.; Cioslowski, J.; Stefanov, B. B.; Liu, G.; Liashenko, A.; Piskorz, P.; Komaromi, I.; Martin, R. L.; Fox, D. J.; Keith, T.; Al-Laham, M. A.; Peng, C. Y.; Nanayakkara, A.; Challacombe, M.; Gill, P. M. W.; Johnson, B.; Chen, W.; Wong, M. W.; Gonzalez, C.; Pople, J. A. *Gaussian 03*; Gaussian, Inc.: Pittsburgh, PA, 2003.

(24) Boys, S. B.; Bernardi, F. *Mol. Phys*. **1970**, *19*, 553.

(25) Luque, F. J.; Orozco, M. *MOPETE-98 computer program*; Universitat de Barcelona: Barcelona, 1998.

(26) Garau, C.; Quiñonero, D.; Frontera, A.; Costa, A.; Ballester, P.; Deyà, P. M. *Org. Lett*. **2003**, *5*, 2227.

(27) (a) Bader, R. F. W. *Chem. Rev*. **1991**, *91*, 893. (b) Bader, R. F. W. *Atoms in Molecules. A Quantum Theory*; Clarendon: Oxford, 1990.

(28) http://www.AIM2000.de (accessed Sep 7, 2007).

(29) Amos, R. D.; Alberts, I. L.; Andrews, J. S.; Colwell, S. M.; Handy, N. C.; Jayatilaka, D.; Knowles, P. J.; Kobayashi, R.; Laidig, K. E.; Laming, A. G.; Lee, M.; Maslen, P. E.; Murray, C. W.; Rice, J. E.; Simandiras, E. D.; Stone, A. J.; Su, M.-D.; Tozer. D. J. *CADPAC*: *The Cambridge Analytic Derivatives Package Issue 6*; Cambridge, U.K., 1995.

(30) Hernandez-Trujillo, J.; Vela, A. *J. Phys. Chem*. **1996**, *100*, 6524.

(31) (a) Cheeseman, J. R.; Carrol, M. T.; Bader, R. F. W. *Chem. Phys. Lett*. **1998**, *143*, 450. (b) Koch, U.; Popelier, P. L. A. *J. Phys. Chem*. **1995**, *99*, 9794. (c) Cubero, E.; Orozco, M.; Luque, F. J. *J. Phys. Chem. A* **1999**, *103*, 315.

CT700122Y